

## Preparation of a new quartz crystal microbalance sensor based on molecularly imprinted nanofilms for amitrole detection

Oğuz Çakır<sup>1</sup>, Fatma Yılmaz<sup>2</sup>, Zübeyde Baysal<sup>3</sup>, Adil Denizli<sup>4,\*</sup>

<sup>1</sup>Dicle University, Science and Technology Application and Research Center, Diyarbakır, Turkey.

<sup>2</sup>Bolu Abant İzzet Baysal University, Chemistry Technology Department, Gerede, Bolu, Turkey.

<sup>3</sup>Dicle University, Faculty of Science, Department of Chemistry, Diyarbakır, Turkey.

<sup>4</sup>Hacettepe University, Department of Chemistry, Beytepe, Ankara, Turkey.

\*corresponding author e-mail address: [denizli@hacettepe.edu.tr](mailto:denizli@hacettepe.edu.tr)

### ABSTRACT

Quartz crystal microbalance (QCM) sensors have been used to detect a variety of biomolecules due to their simplicity, specificity and sensitivity, real-time measurement, low cost and no labeling requirements. A new QCM sensor was prepared by using molecular imprinting method for selective recognition of amitrole. N-metacryloyl-(L)-tryptophan methyl ester (MATrp) was selected as a proper functional monomer and polymerized with ethylene glycol dimethacrylate (EGDMA). Pesticide imprinted poly(ethylene glycol dimethacrylate-N-metacryloyl-(L)-tryptophan methyl ester) [poly(EGDMA-MATrp)] nanofilms were attached to gold surfaces of QCM sensor chips and were characterized by several techniques such as atomic force microscope (AFM), an ellipsometer, FTIR-ATR and contact angle measurements. Kinetic and affinity binding of amitrole was investigated by binding the pesticide imprinted and nonimprinted sensor chips to QCM sensor chips. The imprinted nanofilms were found to show more sensitivity towards the target molecule than the nonimprinted ones. Furthermore, adsorption kinetics were determined by passing pesticide solutions at different concentrations through QCM sensor systems. The most proper model was found to be Langmuir adsorption model for these affinity systems. In addition, competitive adsorption experiments were performed to display selectivity of the pesticide imprinted nanofilms. The prepared sensor was also efficiently applied for the selective detection of amitrole in green pepper.

**Keywords:** *molecular imprinting; sensor; quartz crystal microbalance; amitrole.*

### 1. INTRODUCTION

The pesticides are among the most dangerous compounds in the environment. They are toxic, mobile and capable of bioaccumulation. Nowadays, they are found in all surface waters and in a growing number of aquifers [1]. Their presence in water is considered a potential risk not only for drinking water quality and human health but also for ecosystems [2]. During the last two decades, pesticide usage has increased dramatically and their presence in vegetable, fruits, and environment has increased. Nowadays, the more sensitive detection of pesticides has arisen due to the problem of them faster [3-5]. Herbicides, which are known as one of the pesticides group, are commonly used against crop diseases in agricultural areas. When these chemicals are applied to crops, its droplets are fall on soil, plant, and water. Hence they may be harmful for human when these pesticides are taken directly or indirectly by humans with food and drinking water [6].

Amitrole is a heterocyclic herbicide and derived from triazole (3-amino-1,2,4-triazole) known as aminotriazole. It is a toxic herbicide used to control weeds in agriculture [7,8]. Since its solubility is high in water it can lead to polluted ground and surface water so it may lead to drinking water contamination. This herbicide causes liver cancer in animals [6]. The Environmental Protection Agency (EPA) has prohibited the use of amitrole in food crops due to this effect [9]. Amitrole is often determined by different methods, such as capillary electrophoresis [10,11], SPE-HPLC [12] and electrochemical methods [8,13]. Among the

methods for pesticide detection, molecularly imprinted polymers (MIPs) may be advantageous. These polymers are synthetic materials with specific recognition sites complementary in shape, size and functional groups to the template molecule involving an interaction mechanism based on molecular recognition [14]. MIPs are prepared easily, cheap, stable and can be manufactured in large quantities with good reproducibility [15]. These polymers have been used in many different areas such as, for biological molecules and analytical applications [5,16-18].

In the past years, MIPs have received considerable scientific attention in the field of the sensor [19,20]. In addition, MIPs and the combination of Quartz Crystal Microbalance (QCM) based on microgravimetric analysis have been popular for selective detections [5,21-24]. The QCM sensors are practical tools and measure of small mass changes on the sensor surface. They are specific, sensitive, highly accurate, stable and reproducible. QCM devices are highly suitable for converting the recognition process achieved using MIP-based memories into a sensor signal. Unlike the commonly used method for determination of biomolecules, QCM sensors can measure the interactions of biomolecules without the need for any labeling. The absence of the labeling process saves both time and costs. Furthermore, interactions with other molecules in the environment due to marker molecules may result in incorrect results. These problems are solved by the use of QCM sensors. In addition, the interactions between the analyte and the surface can be measured

in real time and directly by these sensors. Therefore, the combination of a QCM and MIPs as synthetic receptors enhances the sensitivity through MIP process-based multiplexed binding sites using size, 3-D-shape and chemical function having molecular memories of the prepared sensor system toward the target molecule to be detected [25-33].

Herein, we prepared a new amitrole imprinted QCM sensor using MIPs as a recognition material. This sensor was characterized by contact angle, atomic force microscope, and an ellipsometer. Real-time and directly measurement of the interactions between analyte and surface by these sensors provides

## 2. EXPERIMENTAL SECTION

### 2.1. Chemicals.

Amitrole was obtained from Dr. Ehrenstorfer, all other chemicals were of analytical grade purity and purchased from Sigma-Aldrich.

### 2.2. Synthesis of N-methacryloyl-L-tryptophan methyl ester.

The synthesis of N-methacryloyl-L-tryptophan methyl ester (MATrp) was reported previously [34]. In the synthesis reaction, L-tryptophan methyl ester (5.0 g) and hydroquinone (0.2 g) were dissolved in 100 mL of dichloromethane. This solution was cooled to 0 °C. After adding, triethylamine (12.7 g), methacryloyl chloride (5.0 mL) was poured slowly into this solution and then stirred magnetically at room temperature for 2 h. Hydroquinone and unreacted methacryloyl chloride were extracted with a 10% NaOH solution at the end of the chemical reaction,. The aqueous phase was evaporated in a rotary evaporator. The residue (i.e., MATrp) was recrystallized in ethanol.

### 2.3. Preparation of amitrole imprinted QCM sensor.

The gold surfaces were cleaned in a piranha solution (3:1 H<sub>2</sub>SO<sub>4</sub>/H<sub>2</sub>O<sub>2</sub>; v/v) for 5 min before coating. The cleaned surfaces were immersed into 3 M allyl mercaptan for 24 h. The electrode was then washed with ethanol-deionized water (4:1; v/v) for 10 min. For the preparation of amitrole imprinted QCM sensor, MATrp monomer (100 µmol) was formed with amitrole (10 µmol) to obtain pre-complex for 2 h. This complex was mixed with 100 µmol of cross-linker monomer (EGDMA) and 2 mg of initiator (AIBN). Pure nitrogen gas was purged for 15 min to evacuate the air completely since the presence of oxygen would prohibit polymerization. Then, 20 µL of the final monomer solution was dropped onto the gold surface QCM chip. Polymerization was initiated with UV lamp (100 W, 365 nm) for 3 h. The amitrole imprinted QCM sensor was washed with ethanol at the end of the polymerization process. The template was removed with 0.01 M CaCl<sub>2</sub>, then amitrole imprinted sensor was dried. The nonimprinted (NIP) QCM sensor was also prepared with same procedure without template (amitrole) molecule.

Nonimprinted p(EGDMA-MATrp) and amitrole imprinted p(EGDMA-MATrp) nanofilms were characterized by using FTIR-ATR spectroscopy and the results are given below:

3345 cm<sup>-1</sup> (N-H bond), 1728 cm<sup>-1</sup>, 1662 cm<sup>-1</sup> and 1610 cm<sup>-1</sup> (carbonyl C=O), (amide I) and (amid II), respectively. FTIR-ATR spectrum of p(EGDMA-MATrp)-amitrole is given as follows: 1634 cm<sup>-1</sup> (cyclic C-N), 1294 cm<sup>-1</sup> (aryl C-N).

the characterization of the relationship between analyte and ligand as a quantitative analysis or determination of the kinetic, thermodynamic and concentration parameters as a qualitative analysis. So, different concentrations of amitrole were used in QCM-MIPs system and then, detection dynamics and binding kinetics were determined. Selectivity, sensitivity and reusability of the amitrole imprinted QCM sensor were also investigated. Furthermore, the prepared sensor was used for the determination of amitrole in green pepper to evaluate the application of this sensor to real samples.

### 2.4. Characterization of QCM sensor surface.

**2.4.1. Atomic force microscopy measurements.** Atomic force microscope (AFM) was used in tapping mode (Nanomagnetics Instruments, Oxford, England) so that system could perform measurements in high resolution (4096x4096 pixel) due to the cantilever interferometer. Vibration amplitude, free vibration amplitude, and oscillation frequency were 1 VRMS, 2 VRMS and 341.30 kHz, respectively.

**2.4.2. Ellipsometry measurements.** Ellipsometer measurements were achieved by an Auto-nulling imaging ellipsometer (Nanofilm EP3- Nulling Ellipsometry, Germany). A six-zone auto-nulling procedure integrating sample areas was followed by a fitting algorithm in the layer thickness analysis.

**2.4.3. Contact angle measurements.** A KRUSS DSA 100 (Hamburg, Germany) instrument was used for contact angle measurement. For this aim, contact angle values of the unmodified, nonimprinted and amitrole imprinted QCM chips were used. The average of the ten contact angle values of different drops was obtained to calculate contact angle values.

### 2.5. Desorption of amitrole from the QCM chip surface.

Imprinted amitrole was desorbed by the batch system using 0.01 M CaCl<sub>2</sub> solution for 2 h. The amitrole imprinted sensor was then washed with deionized water and dried under vacuum (200 mmHg, 25 °C).

### 2.6. Kinetic analysis and selectivity studies.

The amitrole imprinted and nonimprinted QCM sensors were studied for kinetic analysis. For this aim, amitrole solutions were prepared at different concentrations (0.06-11.9 nM). Firstly, QCM sensor chips were washed with 25 mL of ultrapure water. The surfaces were equilibrated with methanol: distilled water. The amitrole solutions were applied to the QCM system (1 mL/min). The change in resonance frequency was monitored and reached a plateau in 4 min. Then, the desorption reagent was applied to the system, afterward pesticide imprinted sensor was washed with ultrapure water.

Kinetic and equilibrium isotherm coefficients were obtained from equilibrium binding parameter (Scatchard) and Langmuir, Freundlich, and Langmuir-Freundlich adsorption models, respectively. The applied models are as follows:

Equilibrium kinetic analysis

$$d\Delta m/dt = k_a C \Delta m_{max} - (k_a C + k_d) \Delta m \quad (1)$$

Scatchard

$$\Delta m_{equilibrium}/C = K_A \Delta m_{max} - K_A \Delta m_{equilibrium} \quad (2)$$

where  $d\Delta m/dt$  is QCM signal change velocity;  $m$  and  $\Delta m_{max}$  are the measured signal by binding and maximal signal from the increase in mass ( $\text{nM}/\text{cm}^2$ );  $C$  is the pesticide concentration ( $\text{nM}$ );  $k_a$  ( $1/\text{nM}\cdot\text{s}$ ) and  $k_d$  ( $1/\text{s}$ ) are the forward and reverse kinetic rate constants.

Forward equilibrium constant  $K_A$  is calculated from  $\Delta m_{equilibrium}/C - \Delta m_{equilibrium}$  curve graphic. Reverse equilibrium constant  $K_D$  can also be calculated with  $1/K_A$  equation.

Langmuir

$$\Delta m = \{\Delta m_{maks}[C]/(K_D + [C])\} \quad (3)$$

Freundlich

$$\Delta m = \Delta m_{maks}[C]^{1/n} \quad (4)$$

Langmuir-Freundlich

$$\Delta m = \{\Delta m_{maks}[C]^{1/n}/K_D + [C]^{1/n}\} \quad (5)$$

where  $\Delta m_{max}$  ( $\text{nM}/\text{cm}^2$ ) is the maximal QCM signal shift;  $[C]$  is amitrole concentration ( $\text{nM}$ );  $K_A$  ( $1/\text{nM}$ ), and  $K_D$  ( $\text{nM}$ ) are the forward and reverse equilibrium constants, respectively.  $1/n$  is Freundlich exponent.

The selectivity of the amitrole imprinted sensor was studied with competitor pesticides, such as benzotriazole and dinoseb. These competitive compounds ( $11.9 \text{ nM}$ ) interacted with the QCM

sensor chip. The distribution coefficient was determined by Eq (7) to evaluate the binding specificity of the amitrole imprinted sensor.

$$K_d = [(C_i - C_f)/C_f] \times V/m \quad (6)$$

where  $K_d$  ( $\text{mL}/\text{g}$ ) is the distribution coefficient;  $C_i$  ( $\text{nM}$ ) and  $C_f$  ( $\text{nM}$ ) refer to the pesticide solution concentrations before and after binding;  $V$  ( $\text{mL}$ ) and  $m$  ( $\text{g}$ ) are the pesticide solution volume and the mass of nanofilm, respectively.

The selectivity coefficient ( $k$ ) for the binding of amitrole in the presence of competitor pesticides can be obtained from equilibrium binding data constant to

$$k = \Delta m_{template}/\Delta m_{competitor} \quad (7)$$

The relative selectivity coefficient ( $k'$ )

$$k' = k_{imprinted}/k_{nonimprinted} \quad (8)$$

### 2.6. Amitrole determination from natural source with QCM sensor.

Amitrole detection from a natural source was also carried out by using freshly prepared green pepper. For this purpose, green pepper was homogenized by broking stainless steel blends in an ice bath and diluted to 50% (v/v) with methanol-pure water. The diluted green pepper centrifuged at  $4^\circ\text{C}$  at  $10,000 \text{ rpm}$  for  $30 \text{ min}$ . Sample solution was interacted with QCM sensor a peristaltic pump by passing through  $0.22 \mu\text{m}$  syringe filters and determined to QCM sensor responses.

## 3. RESULTS SECTION

### 3.1. Characterization of amitrole imprinted QCM sensor.

The amitrole imprinted QCM sensor was characterized by contact angle, AFM and ellipsometer measurements. Figure 1.a and Figure 1.b show the AFM images of nonimprinted p(EGDMA-MATrp) and amitrole imprinted of p(EGDMA-MATrp)-amitrole sensor surface respectively. According to AFM images, the surface depth of amitrole imprinted QCM sensor chip was found to be  $120.67 \pm 0.93 \text{ nm}$ . Because of depth values and thickness differences between nonimprinted ( $80.31 \pm 2.41 \text{ nm}$ ) and amitrole imprinted QCM sensor we can say that the imprinting procedure was achieved.

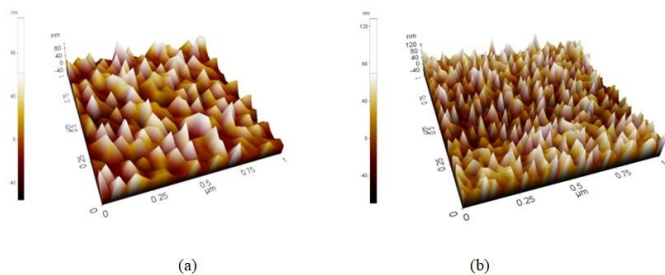


Fig. 1. The atomic force microscopy images of a) nonimprinted and b) Amitrole imprinted QCM sensor surfaces.

On the other hand, the roughness of the surface is well distributed through the surface of the sensor, which indicates that amitrole imprinting on the QCM sensor chip has been homogeneously achieved. This property is one of the important parameters controlling the specificity, selectivity and recognition rate of the sensor [5].

After the imprinting process, ellipsometer measurements have been carried out for determination of the thickness of the amitrole imprinted sensor. According to the results, the thickness of nonimprinted ( $131.3 \pm 3.74 \text{ nm}$ ) and imprinted ( $135.5 \pm 1.0$ ) sensors obviously show that polymeric nanofilms are desirable for sensitive recognition in QCM sensors. Figure 2.a and Figure 2.b show the thickness values of the amitrole imprinted and nonimprinted sensors by using ellipsometer.

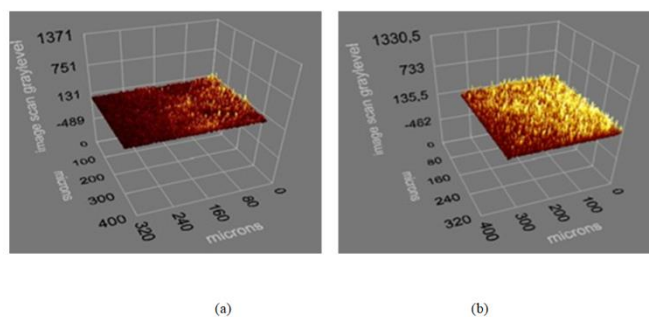


Fig. 2. Ellipsometer images of a) nonimprinted and b) Amitrole imprinted QCM sensor surfaces.

Contact angles were also measured. The contact angle values of unmodified, nonimprinted and amitrole imprinted QCM sensor chips were found to be  $60.2^\circ \pm 0.24$ ,  $68.3^\circ \pm 0.47$  and  $72.4^\circ \pm 0.12$ , respectively. The increase of contact angle values may be due to the increase in hydrophobic character by MATrp which is a functional monomer and hydrophobic template molecule amitrole (Figure 3.a and Figure 3.b).

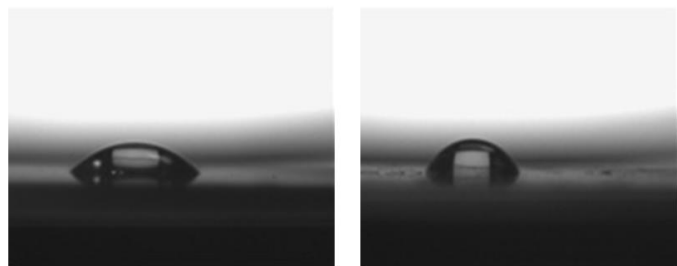


Fig. 3. Contact angle measurements of a) nonimprinted and b) Amitrole imprinted QCM sensor surfaces.

### 3.2. Real-time monitoring of responses of the amitrole imprinted QCM sensor.

The QCM sensor chip was prepared for real-time detection of amitrole in aqueous solution in the concentration range from 0.06 to 11.9 nM. When the amitrole solution reached to the sensor surface, amitrole imprinted QCM sensor had quick responses. The increase of amitrole concentration caused an increase in the amitrole imprinted QCM sensor response, as expected. The total measurement time was read as 25 min (Figure 4).

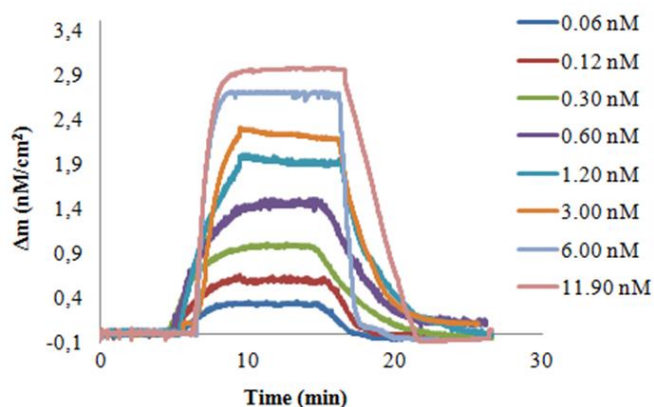


Fig. 4. The real-time Amitrole detection chart (Mass (nM/cm<sup>2</sup>)-Time) by Amitrole imprinted QCM sensor at different concentrations.

### 3.3. Kinetic and adsorption isotherm studies.

Scatchard model is used to determine the binding and equilibrium kinetic analysis. After calculation of curve slopes and plotting against to concentrations,  $K_A$ ,  $K_D$ ,  $k_a$  and  $k_d$  values were calculated by applying equilibrium and binding kinetic analysis. The results are given in Table 1. The association constant  $K_A$  for the binding of amitrole to the sensor was found to be 1.978 nM<sup>-1</sup>, indicating that the affinity of the binding sites is very strong.

Langmuir, Freundlich and Langmuir-Freundlich adsorption isotherm models were used for surface homogeneity and interaction selectivity of the QCM sensor. The Langmuir adsorption isotherm model is usually used to fit molecular imprinting binding isotherms. The Freundlich adsorption isotherm model is generally relevant to a heterogeneous model. The Langmuir-Freundlich adsorption isotherm model contributes heterogeneity information about adsorption behavior over wide concentration regions [5]. In our study, Langmuir adsorption isotherm model was the best-fitted model among these adsorption isotherm models for amitrol ( $R^2 = 0.985$ ,  $\Delta m_{max} = 2.433$  nM/cm<sup>2</sup>) (Table 1). These results clearly show that the binding of amitrole onto amitrole imprinted QCM sensor is a monolayer.

Table 1. Kinetic and isotherm parameters.

	Equilibrium analysis (Scatchard)	Association kinetics analysis	Langmuir	Freundlich	Langmuir-Freundlich
$\Delta m_{max}$	1.884	$k_a$ , nM <sup>-1</sup> .s <sup>-1</sup>	0.025	$\Delta m_{max}$	2.433
$K_A$	1.978	$k_d$ , s <sup>-1</sup>	0.164	$\Delta m_{max}$	2.553
$K_D$	0.506	$K_A$ , nM <sup>-1</sup>	0.152	1/n	0.406
$R^2$	0.959	$K_D$ , nM	6.560	$R^2$	0.915
		$R^2$	0.956	$K_A$	4.348
				1/n	0.406
				$K_D$	0.243
				$R^2$	4.113
				$R^2$	0.953

### 3.4. The selectivity of amitrole imprinted QCM sensor.

The selectivity of amitrole imprinted QCM sensor was investigated for the better understanding of the specificity of the interactions between the binding sites of the MIP-QCM sensor and template molecule. For this aim, benzotriazole and dinoseb were used as a competitor agent. Table 2 shows the selectivity coefficients for the amitrole imprinted and nonimprinted QCM sensor and the relative selectivity coefficients. The obtained results showed that amitrole recognition site has been created during the imprinting process and cavities created in the amitrole imprinted QCM sensor recognized pesticide preferentially. No defined cavities exist to provide selective binding of amitrole with NIP-QCM sensor. The selectivity comparison of amitrole imprinted sensor with benzotriazole and dinoseb was given in Figure 5. Herein MATrp, which is an amino acid based functional monomer, assembled around the template molecule via interaction with functional groups on amitrole structure, leaving behind a selective binding site after polymerization. The relative selectivity coefficient for amitrole showed that the cavities created in the pesticide imprinted QCM sensor recognized imprinted template molecule and had structural memory and remarkable molecular size matching for template molecule.

Table 2. Selectivity coefficients of amitrole imprinted and nonimprinted QCM sensors.

	Molecular Imprinted		Nonimprinted		
	$\Delta m$	k	$\Delta m$	k	k'
Amitrole	2.83	-	0.033	-	-
Dinoseb	0.106	26.698	0.026	1.269	21.035
Benzotriazole	0.124	22.823	0.019	1.737	13.14

Özkütük et al. [21] have studied the ligand exchange based paraoxon imprinted QCM sensor. The frequency of sensor has decreased after adding the paraoxon solution, then has reached the constant value in 30 min. In our study, the response time of amitrole imprinted sensor is 25 min. It is relatively quick compared to the above study. On the other hand, the response time of paraoxon imprinted QCM sensor has been found to be 20 min in their another study [35].

### 3.5. Reusability studies.

The reusability of amitrole imprinted QCM sensor was investigated by six cycles. For this aim, 0.595 nM amitrole solution interacted with amitrole imprinted sensor consecutively. The sensor was washed with 0.1 M CaCl<sub>2</sub> + 1% acetic acid mixture solution and deionized water until the frequency reached a constant value. As seen in Figure 6, there was a slight difference in the frequency shift. Thus, we concluded that the amitrole imprinted QCM sensor can be reused successfully with reproducible results for amitrole solutions.

### 3.6. Analysis of green pepper.

Amitrole imprinted QCM sensor was also used to detect amitrole in a natural source (green pepper). The prepared sample solutions interacted with amitrole imprinted QCM sensor via a peristaltic pump by passing through 0.22 μm syringe filters. Freshly prepared green pepper samples caused an increase in

sensor response as expected by remaining between calibration points. As it is shown in Figure 7, amitrole concentration was approximately 0.342 nM (28.69 ng/L) in green pepper. As a conclusion, amitrole imprinted sensor has an ability to detect amitrole in a natural complex mixture, namely, green pepper.

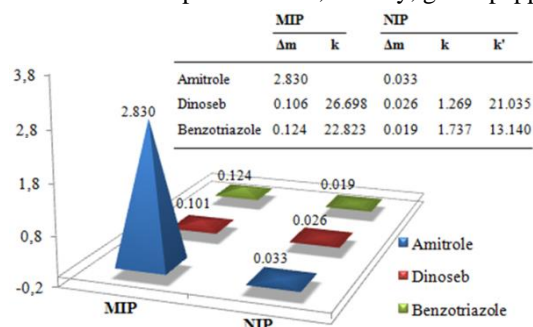


Fig. 5. The selectivity comparison studies of amitrole imprinted sensor with dinoseb and benztiazazole.

#### 4. CONCLUSIONS

In this study, we prepared a new QCM sensor for real-time amitrole detection. The sensor was prepared by the modification of the gold surface of QCM sensor with the amitrole imprinted nanofilm and characterized with AFM and ellipsometer. The nanofilm was prepared with p(EGDMA-MATrp) in the absence and presence of amitrole and characterized by FTIR-ATR. The Scatchard, Langmuir, Freundlich and Langmuir-Freundlich models were used for binding, equilibrium and adsorption kinetics. It was found that Langmuir adsorption model best fitted

#### 5. REFERENCES

- [1] Kouzayha A., Rabaa A.R., Iskandarani M., Beh D., Budzinski H., Jaber F., Multi residue method for determination of 67 pesticides in water samples using solid-phase extraction with centrifugation and gas chromatography-mass spectrometry, *Am. J. Anal. Chem.*, 3, 257-265, **2012**.
- [2] Bailey H., Deanovic L., Rayes E., Kimball T., Larson K., Cortright K., Conner V., Hinton D.E., Diazinon and chlorpyrifos in urban waterways in Northern California USA, *Environ. Toxicol. and Chem.*, 19, 82-87, **2000**.
- [3] Zhou J., Ma C., Zhou S., Ma P., Chen F., Qi Y., Chen H., Preparation, evaluation and application of molecularly imprinted solid-phase microextraction monolith for selective extraction of pirimicarb in tomato and pear, *J. Chromatogr. A.*, 1217, 7478-7483, **2010**.
- [4] Kim N., Park I.S., Kim D.K., High-sensitivity detection for model organophosphorus and carbamate pesticide with quartz crystal microbalance-precipitation sensor, *Biosens. Bioelectron.*, 22, 1593-1599, **2007**.
- [5] Saylan Y., Akgönüllü S., Çimen D., Derazshamshir A., Bereli N., Yılmaz F., Denizli A., Development of surface plasmon resonance sensors based on molecularly imprinted nanofilms for sensitive and selective detection of pesticides, *Sens. Act. B.*, 241, 446-454, **2017**.
- [6] Tuna S., Duman O., Soylu I., Kancı Bozoğlan B., Spectroscopic investigation of the interactions of carbofuran and amitrol herbicides with human serum albumin, *J. Lumin.*, 151, 22-28, **2014**.
- [7] Ensafi A.A., Amini M., Rezaei B., Biosensor based on ds-DNA decorated chitosan modified multiwalled carbon nanotubes for voltammetric biodetection of herbicide amitrol, *Colloid. Surface B.*, 109, 45-51, **2013**.
- [8] Siswana M., Ozoemena K., Nyokong T., Electrocatalytic detection of amitrole on the multi-walled carbon nanotube-iron(II) tetra-aminophthalocyanine platform, *Sensors B.*, 8, 5096-5105, **2008**.

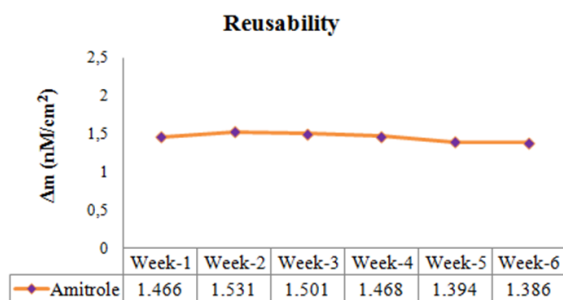


Fig. 6. Reusability of amitrole imprinted QCM sensor.

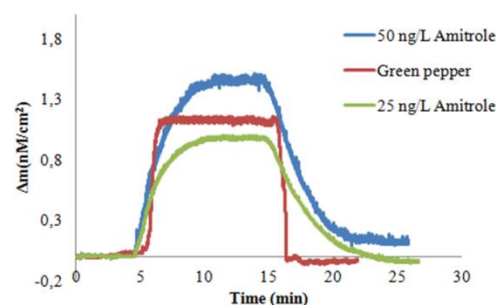


Fig. 7. Amitrole analysis in green pepper by amitrole imprinted QCM sensor.

for amitrole imprinted QCM sensor. The selectivity studies showed that the selectivity coefficients of the p(EGDMA-MATrp)-amitrole complex with respect to benztiazazole and dinoseb are 22.823 and 26.698, respectively. In the light of obtained data, by using the amitrole imprinted QCM sensor system as the recognition material, a novel amitrole imprinted sensor with high sensitivity, selectivity and short response time can be used for the determination of amitrol as a potential alternative to determination of pesticides.

- [9] Moreno M., Bermejo E., Sanchez A., Chicharro M., Zapardiel A., Application of matrix solid-phase dispersion to the determination of amitrole and urazole residues in apples by capillary electrophoresis with electrochemical detection, *Anal. Bioanal. Chem.*, 39, 867-872, **2008**.
- [10] Chiccarro M., Moreno M., Bermejo E., Ongay S., Zapardiel A., Determination of amitrole and urazole in water samples by capillary zone electrophoresis using simultaneous UV and amperometrical detection, *J. Chromatogr. A.*, 1099, 191-197, **2005**.
- [11] Lucarelli F., Kicela A., Palchetti I., Marrazza G., Mascini M., Electrochemical DNA biosensor for analysis of wastewater samples, *Bioelectrochem.*, 58, 113-118, **2002**.
- [12] Bobeldijk I., Bioess K., Speksnijder P., van Leer dam T., Determination of the herbicide amitrole in water with pre-column derivatization, liquid chromatography and tandem mass spectrometry, *J. Chromatogr. A.*, 938, 15-22, **2001**.
- [13] Sanchez Bayo F., Hyne R.V., Desseille K.L., An amperometric method for the detection of amitrole, glyphosate and its aminomethyl-phosphonic acid metabolite in environmental waters using passive samplers, *Anal. Chim. Acta*, 675, 125-131, **2010**.
- [14] Pichon V., Chapuis-Hugon F., Role of molecularly imprinted polymers for selective determination of environmental pollutants- A review, *Anal. Chim. Acta*, 622, 148-161, **2008**.
- [15] Bereli N., Saylan Y., Uzun L., Say R., Denizli A., L-histidine imprinted supermacroporous cryogels for protein recognition, *Sep. Purif. Technol.*, 82, 28-35, **2011**.
- [16] Saylan Y., Üzek R., Uzun L., Denizli A., Surface imprinting approach for preparing specific adsorbent for IgG separation, *J. Biomater. Sci. Polym. Ed.*, 25, 881-894, **2014**.

- [17] Rabieizadeh M., Kashefifomrad S.M., Naeimpoor F., Monolithic molecularly imprinted cryogel for lysozyme recognition, *J. Sep. Sci.*, 37, 2983-2990, **2014**.
- [18] Gültekin A., Ersöz A., Denizli A., Say R., Preparation of new molecularly imprinted nanosensor for cholic acid determination, *Sens. Act. B.*, 162, 153-158, **2012**.
- [19] Ersöz A., Diltemiz S.E., Özcan A.A., Denizli A., Say R., 8-OHdG sensing with MIP based solid phase extraction and QCM technique, *Sens. Act. B.*, 137, 7-11, **2009**.
- [20] Chen Y.C., Brazier J.J., Yan M.D., Bargo P.R., Prahl S.A., Fluorescence-based optical sensor design for molecularly imprinted polymers, *Sens. Act. B.*, 102, 107-116, **2004**.
- [21] Özkütük E.B., Diltemiz S.E., Özalp E., Say R., Ersöz A., Ligand exchange based paraoxon imprinted QCM sensor, *Mat. Sci and Eng. C.*, 33, 938-942, **2013**.
- [22] Vila M.A., Zougagh M., Escarpa A., Ios A.R., Supported liquid membrane-modified piezoelectric flow sensor with molecularly imprinted polymer for the determination of vanillin in food samples, *Talanta*, 72, 1362-1369, **2007**.
- [23] Atay S., Pişkin K., Yılmaz F., Çakır C., Yavuz H., Denizli A. A., Quartz crystal microbalance based biosensors for detecting highly metastatic breast cancer cells, *Anal. Methods*, 8, 153-161, **2016**.
- [24] Bakhshpour M., Özgür E., Bereli N., Denizli A., Microcontact imprinted quartz crystal microbalance nanosensor for protein C recognition, *Colloids Surfaces B.*, 151, 264-270, **2017**.
- [25] Diltemiz S.E., Keçili R., Ersöz A., Say R., Molecular imprinting technology in Quartz Crystal Microbalance (QCM) sensors, *Sensors*, 17, 454, **2017**.
- [26] Shaikh H., Memon N., Bhanger M.I., Nizamani S.M., Denizli A., Magnetic molecularly imprinted polymer based solid phase microextraction fiber for ultratrace analysis of endosulfan I and II in real aqueous matrix through GC- $\mu$ ECF, *J. Chromatogr. A.*, 1337, 179-187, **2014**.
- [27] Shaikh H., Andaç M., Memon N., Bhanger M.I., Nizamani S.M., Denizli A., Synthesis and characterization of molecularly imprinted polymer embedded composite cryogel discs: application for the selective extraction of cypermethrins from aqueous samples prior to GC-MS analysis, *RSC Adv.*, 5, 26604-26615, **2015**.
- [28] Jha S.K., Hayashi K., A quick responding quartz crystal microbalance sensor array based on a molecular imprinted polyacrylic acids coating for selective identification of aldehydes in body odor, *Talanta*, 134, 105-119, **2015**.
- [29] Cheng X., Zhang Q., Li S.F.Y., Liu B., Molecularly imprinted polymer-coated quartz crystal microbalance for detection of parathion, *Malaysian J. Anal. Sci.*, 21, 1327-1334, **2017**.
- [30] Yun Y., Pan M., Fang G., Gu Y., Wen W., Xue R., Wang S., An electrodeposited molecularly imprinted quartz crystal microbalance sensor sensitized with AuNPs and rGO material for highly selective and sensitive detection of amantadine, *RSC Adv.*, 8, 6600-6607, **2018**.
- [31] Ayankajo A.G., Reut J., Boroznjak R., Öpik A., Syritski V., Molecularly imprinted poly(Meta-phenylenediamine) based QCM sensor for detecting Amoxicillin, *Sensor Actuat B: Chemical*, 258, 766-774, **2018**.
- [32] Fang G., Yang Y., Zhu H., Qi Y., Liu J., Liu H., Wang S., Development and application of molecularly imprinted quartz crystal microbalance sensor for rapid detection of metolcarb in foods, *Sensor Actuat B: Chemical*, 251, 720-728, **2017**.
- [33] Battal D., Akgönüllü S., Yalçın S.M., Yavuz H., Denizli A., Molecularly imprinted polymer based quartz crystal microbalance sensor system for sensitive and label-free detection of synthetic cannabinoids in urine, *Biosens. Bioelectron.*, 111, 10-17, **2018**.
- [34] Demirçelik A.H., Perçin I., Denizli A., Supermacroporous hydrophobic affinity sorbents for penicillin acylase purification, *J. Macromol. Sci. A.*, 54, 71-79, **2017**.
- [35] Özkütük E.B., Diltemiz S.E., Özalp E., Ersöz A., Say R., Silan based paraoxon memories onto QCM electrodes, *J. Ind. Eng. Chem.*, 19, 1788-1792, **2013**.

## 6. ACKNOWLEDGEMENTS

This work has been supported by the Scientific and Technological Research Council of Turkey and was assigned Project number: 115Z126.

© 2018 by the authors. This article is an open access article distributed under the terms and conditions of the Creative Commons Attribution license (<http://creativecommons.org/licenses/by/4.0/>).